

Multinuclear Magnetic Resonance Tracking of Hydro, Thermal and Hydrothermal Decomposition of $\text{CH}_3\text{NH}_3\text{PbI}_3$

Abdelrahman M. Askar,^{1†} Guy M. Bernard,^{2†} Benjamin Wiltshire,¹ Karthik Shankar^{1,3} and Vladimir K. Michaelis^{2*}

1- Department of Electrical and Computer Engineering, University of Alberta, Edmonton, Alberta, Canada, T6G 1H9

2- Department of Chemistry, University of Alberta, Edmonton, Alberta, Canada, T6G 2G2

3- NRC National Institute for Nanotechnology, Edmonton, Alberta, Canada, T6G 2M9

† - Authors contributed equally

* Corresponding author: vladimir.michaelis@ualberta.ca

Abstract

An NMR investigation of methylammonium lead iodide, the leading member of the hybrid organic-inorganic perovskite class of materials, and of its putative decomposition products as a result of exposure to heat and humidity, has been undertaken. We show that the ^{207}Pb NMR spectra of the compound of interest and of the proposed lead-containing decomposition products, $\text{CH}_3\text{NH}_3\text{PbI}_3\cdot\text{H}_2\text{O}$, $(\text{CH}_3\text{NH}_3)_4\text{PbI}_6\cdot 2\text{H}_2\text{O}$ and PbI_2 , have distinctive chemical shifts spanning over 1400 ppm, making ^{207}Pb NMR an ideal tool for investigating this material; further information may be gained from ^{13}C and ^1H NMR spectra. As reported in many investigations of $\text{CH}_3\text{NH}_3\text{PbI}_3$ on films, the bulk material hydrates in the presence of high relative humidity (approximately 80 %), yielding the monohydrated perovskite $\text{CH}_3\text{NH}_3\text{PbI}_3\cdot\text{H}_2\text{O}$. This reaction is reversible by heating the sample to 341 K. We show that neither $(\text{CH}_3\text{NH}_3)_4\text{PbI}_6\cdot 2\text{H}_2\text{O}$ nor PbI_2 are observed as decomposition products and that, in contrast to many studies on $\text{CH}_3\text{NH}_3\text{PbI}_3$ films, the bulk material does not decompose or degrade beyond $\text{CH}_3\text{NH}_3\text{PbI}_3\cdot\text{H}_2\text{O}$ upon prolonged exposure to humidity at ambient temperature. However, exposing $\text{CH}_3\text{NH}_3\text{PbI}_3$ concurrently to heat and humidity, or directly exposing it to liquid water, leads to the irreversible formation of PbI_2 . In spite of its absence among the decomposition products, the response of $(\text{CH}_3\text{NH}_3)_4\text{PbI}_6\cdot 2\text{H}_2\text{O}$ to heat was also investigated. It is stable at temperatures below 336 K but then rapidly dehydrates, first to $\text{CH}_3\text{NH}_3\text{PbI}_3\cdot\text{H}_2\text{O}$, then to $\text{CH}_3\text{NH}_3\text{PbI}_3$. The higher stability of the bulk material as reported here is a promising advance, since stability is a major concern in the development of commercial applications for this material.

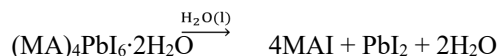
1.) Introduction:

Methylammonium lead halide perovskites ($\text{CH}_3\text{NH}_3\text{PbX}_3$, $\text{X} = \text{I}, \text{Br}, \text{Cl}$, referred to as MAPbX_3 herein) have emerged as the basis of a revolutionary new class of photovoltaic materials since 2009.¹ In the past six years, the photoconversion efficiency (PCE) of perovskite-based solar cells (PSCs) has increased rapidly from 3.8% to $> 20\%$,²⁻⁵ such that it is approaching the record efficiency reported for single-junction monocrystalline Si solar cells. The rapid enhancement in PCE for MAPbX_3 and related PSCs over this short period of time has prompted intense worldwide research efforts, creating a paradigm shift within the photovoltaic research field, providing industry with a material that is approaching the optimal bandgap of single-junction solar cells while avoiding the synthetic complexity associated with high-performance conjugated organic semiconductors.⁶

There has been particular interest in methylammonium lead iodide, MAPbI_3 , which exhibits a bandgap of 1.6 eV,⁷ mainly because of its desirable properties, such as high optical absorption coefficients,⁸ long balanced charge carrier diffusion lengths,⁹⁻¹⁰ as well as the low-cost solution-processing techniques used to incorporate it in solar cells.¹¹ However, despite the promising PCE of MAPbI_3 -based PSCs, they suffer from instability upon prolonged exposure to humid environments, leading to rapid degradation of solar cell performance, which has hindered the commercialization of this new technology thus far. The sensitivity of MAPbI_3 to moisture was discovered in the early stages of PSC development,¹² where exposure of the PSC to a relative humidity (RH) of 35% led to a more than 50% degradation in the PCE of MAPbI_3 solar cells within a few days. Leguy et al. proposed the following equation to describe the reaction of MAPbI_3 with humidity:¹³



These authors suggested that an excess of water may lead to an irreversible degradation product:



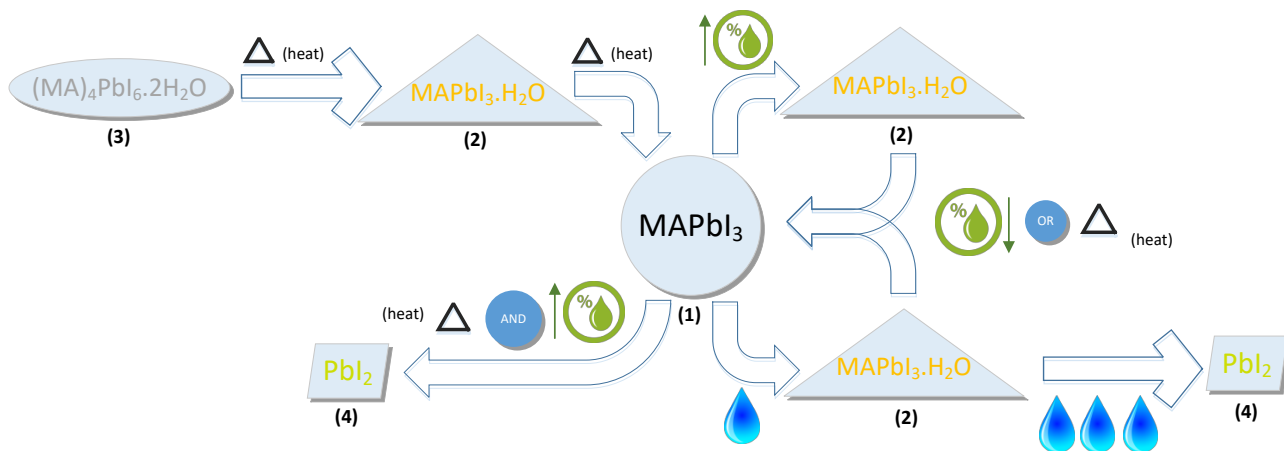
Interestingly, recent studies showed a counter effect, where preparation of the PSC under moderate RH improved PCE.^{14, 15, 16, 17}

Elucidating the exact degradation mechanisms and routes upon exposure of perovskite materials (especially MAPbI₃) to humidity has been the focus of many recent studies, both experimentally and theoretically.¹⁸⁻²⁵ Different analytical techniques have been applied in these investigations, including *in-situ* and time-resolved powder and single-crystal X-ray diffraction (XRD),^{11, 12, 14, 26} optical absorption,¹⁴ and spectroscopic ellipsometry.²⁷ Due to the different humidity conditions being examined (e.g., with/without light, with/without heat, varying humidity levels, etc.) as well as the different ways the perovskite films are prepared in these studies and the varying structures of the devices under investigation, the results are ambiguous, and different degradation pathways of the perovskite materials have been proposed. For instance, earlier studies suggested that solar cell performance degraded as a consequence of the slow decomposition of MAPbI₃ to PbI₂ in addition to MAI or CH₃NH₂ plus HI.²⁸⁻³¹ Recently, an intermediate by-product of MAPbI₃ decomposition, (MA)₄PbI₆·2H₂O³² (i.e., the perovskite dihydrate), was identified by Kamat and co-workers³³ after exposure of an MAPbI₃ film to high RH (90%) for several days in the dark, but these authors did not observe PbI₂. Using *in-situ* grazing incidence XRD (GIXRD), Kelly et al.²⁴ noticed the formation of new peaks in the GIXRD pattern during the decomposition of MAPbI₃ at high RH (80%); these peaks could not be associated with either MAPbI₃ nor PbI₂ and thus were attributed to the formation of (MA)₄PbI₆·2H₂O. The conclusion in these earlier studies of the presence of the perovskite dihydrate was based on comparisons between the XRD pattern of the decomposition product they measured and either the calculated pattern of the dihydrate or the pattern of a synthesized perovskite hydrate, assumed to be the dihydrate. This decomposition product was later

confirmed to in fact be the monohydrate perovskite ($\text{CH}_3\text{NH}_3\text{PbI}_3 \cdot \text{H}_2\text{O}$) by Leguy et al.¹³ Other studies have confirmed the formation of the monohydrate as an intermediate decomposition product, but it is unclear whether this is the final decomposition product or whether the formation of the monohydrate is followed by formation of the dihydrate, and finally of PbI_2 .^{13, 19, 21, 22, 27} These studies focused mainly on either *in* or *ex situ* investigations of the degradation of the perovskite *film*, prepared by various techniques such as solution-processing or co-evaporation, with the MAPbI_3 as the light harvesting layer in different solar cell architectures (i.e., having the perovskite layer deposited on some electron- or hole- transport layer). The varying techniques explain the different conclusions reached by the investigators but unfortunately hinder the determination of the intrinsic interaction mechanisms between the perovskite material and H_2O molecules in a humid environment.

The logic of investigating the material in its operating architecture is indisputable, but a detailed study of the bulk properties of the compounds of interest informs on the ambiguities inherent in the earlier studies and guides future developments. The Kamat group²⁵ recently published a detailed review of spectroscopic and structural techniques that can be employed to monitor the response of perovskites exposed to moisture. Here, we report a solid-state ^{207}Pb , ^{13}C and ^1H nuclear magnetic resonance investigation of bulk samples of MAPbI_3 and its proposed decomposition products. Solid-state nuclear magnetic resonance (NMR) spectroscopy, which probes the local chemical structure in a non-destructive manner, is ideal to identify changes within molecular and periodic solids that affect the structure, composition and optoelectronic properties of these next generation photovoltaic materials. ^{207}Pb nuclei have reasonably receptive $I = 1/2$ nuclear spin, with a moderate resonance frequency (≈ 20.92 %), a natural abundance of 22.1 % and one of the largest known NMR chemical shift ranges, approximately 17,000 ppm,³⁴ making it extremely sensitive to subtle changes within the local Pb chemical and coordination environment.³⁴⁻³⁷ Thus ^{207}Pb NMR is an excellent analytical tool for atomic-level characterization.

In the work presented here, we characterize and highlight the distinct differences between MAPbI₃ and the three proposed Pb-based decomposition products occurring as a consequence of exposure of the former to humid or thermal environments, or both, in the dark (Scheme 1). Our goal is to elucidate the conditions leading to different decomposition pathways, to identify intermediate and final degradation products, and to investigate conditions under which MAPbI₃ may be recovered from these products. We show that solid-state ²⁰⁷Pb NMR spectroscopy is ideally suited to monitor environmental effects on MAPbI₃ and its decomposition products. The results of these measurements, performed on bulk samples, are compared to those obtained on thin-film samples.



Scheme 1: Degradation reaction pathway of MAPbI₃ into three different pseudo-octahedral Pb – I crystalline solid complexes.

2.) Experimental:

2.1) Chemicals and Reagents

Starting materials were obtained from commercial sources: lead (II) iodide (99 %) from Acros Organics (Morris Plains, NJ, USA); methylammonium iodide from Dyesol Limited (Australia); γ -butyrolactone (GBL) (> 99 %) from Sigma-Aldrich (St. Louis, MO, USA); lead (II)

nitrate (> 99 %) from Fisher Scientific (Pittsburgh, PA, USA), and used as received without any further purification.

2.2) Syntheses

Methylammonium lead iodide, $CH_3NH_3PbI_3$ (MAPbI₃)

Single crystals of MAPbI₃ were prepared by the inverse-temperature solubility method developed by Saidaminov.³⁸ A 1.3 M solution of methylammonium iodide (MAI) and PbI₂ in GBL was dissolved at 333 K, filtered and then heated to 389 K where crystallization of MAPbI₃ occurs. After two hours the crystals, which were 7-8 mm across, were removed from the solution, rinsed quickly with GBL, and dried with nitrogen gas. The crystals were kept in a desiccator to inhibit hydration.

Methylammonium lead iodide monohydrate, $CH_3NH_3PbI_3 \cdot H_2O$ (monohydrate)

The perovskite-monohydrate powder was synthesized as reported by Christians et al.³³ A 0.2 M aqueous solution of Pb(NO₃)₂ was added dropwise at room temperature with a 1.2 M aqueous solution of MAI. The solution was left for 18 hours until a pale yellow precipitate formed. The precipitate was filtered, vacuum dried and sealed, protecting it from dehydrating to MAPbI₃.

Methylammonium lead iodide dihydrate, $(CH_3NH_3)_4PbI_6 \cdot 2H_2O$ (dihydrate)

Methylammonium lead iodide dihydrate was synthesized in films using a spin-coating method developed by Halder et al.³⁹ A 1:4 (M/M) solution of PbI₂:MAI was dissolved in DMF and spin-coated at 2000 rpm. The films were then heated at 283 K for five minutes and then cooled in a humid atmosphere (RH = 85%). After 20 minutes, the dihydrate films were a slightly transparent grey color.

2.3) Powder X-Ray Diffraction (XRD)

Powder X-ray diffraction (XRD) was used to verify that the desired products had been synthesized (*vide infra*). Powder patterns were obtained on a Bruker AXS D8 diffractometer using a Cu-K α radiation source. A 2D detector was used for scanning of the 2θ angles. For MAPbI₃, the monohydrate and PbI₂, a fine powder was prepared and XRD was carried out with Omega = 5°. Due to its sensitivity to air and humidity, the monohydrate was sealed in a 1 mm diameter capillary prior to acquisition of XRD data. The XRD measurements for the dihydrate were carried out on thin films spin-coated on a glass substrate. All humidity- and heat-treated samples were handled as described for the monohydrate.

2.4) Solid-State Nuclear Magnetic Resonance Spectroscopy

Room-temperature ²⁰⁷Pb NMR spectra were obtained at 7.05 and 11.75 T on Bruker Avance 300 and 500 NMR spectrometers, respectively, with the former being the preferred option since at 11.75 T the ²⁰⁷Pb NMR signals from the samples of interest appear near that for a local FM radio station (104.9 MHz). All spectra were acquired using 4 mm Bruker NMR probes operating in double resonance mode; unless otherwise noted, spectra were acquired under non-spinning conditions using a Hahn-echo with ²⁰⁷Pb $\gamma B_1/2\pi$ of 65 kHz and two-pulse phase modulated (TPPM)⁴⁰ high-power ¹H decoupling ($\gamma B_1/2\pi = 62.5$ kHz). The ²⁰⁷Pb spin-lattice relaxation (T_1) times were determined for each sample using a modified inversion recovery sequence incorporating a refocusing pulse; i.e., $\pi - \tau_1 - \pi/2 - \tau_2 - \pi/2 - \tau_2 - \text{ACQ}$, where τ_1 is the variable delay used to assess the inversion recovery and τ_2 is the delay typically used in the solid-echo sequence (30 μs for the work presented here). Reported T_1 values were obtained by fitting the peak intensity of the maxima or minima to an exponential decay function (*i.e.*, a three parameter fit). Recycle delays for each sample were based on the T_1 values obtained from these measurements; when more than one crystalline species was present, the recycle delay was based on the greatest T_1 value of the observed species. All ²⁰⁷Pb NMR

spectra were referenced to $\text{Pb}(\text{CH}_3)_4$ (0 ppm) by setting the isotropic value for the ^{207}Pb chemical shift of non-spinning $\text{Pb}(\text{NO}_3)_2$ to -3491.6 ppm; the value reported by Neue et al.⁴¹ was used, with a correction for the different chemical shifts expected due to the lower temperature in our lab (294 K rather than 295 K for Neue et al.)

Lead-207 NMR spectra were also obtained as described above with temperatures in the 294 to 350 K range on the Avance 500 NMR spectrometer; temperatures were regulated using the Bruker hardware, but the actual temperatures were calibrated with the ^{207}Pb chemical shifts of $\text{Pb}(\text{NO}_3)_2$.^{42,}
⁴³ To avoid pressure build up from the possible evolution of gases at elevated temperatures, the standard rotor cap was replaced with one that had a 0.5 mm hole drilled through it.

The ^{207}Pb NMR powder patterns for the monohydrate were broad and asymmetric (*vide infra*). To avoid potential line shape distortions, some variable-offset cumulative spectra (VOCS)⁴⁴ were acquired with the offset varied in 30 kHz increments for three (7.05 T) or five (11.75 T) steps. These spectra are displayed using the skyline projection method.⁴⁵ Although VOCS obtained at 7.05 T were not significantly different from spectra obtained in a single step, we found that at higher fields the technique was necessary to obtain spectra with the proper breadth and lineshape. Obtaining variable-offset spectra was not always practical, but because of the distinctive line shape of the ^{207}Pb spectra for the monohydrate, it could readily be identified even if it was acquired in a single step for surveying purposes at 7.05 T.

Carbon-13 NMR spectra with magic-angle spinning (MAS) were obtained with cross-polarization (CP)⁴⁶ and a spinning frequency of 5.0 kHz. A $4.0 \mu\text{s}$ ^1H 90° pulse, a 5 ms contact time, an acquisition time of 35 ms and a 60 s recycle delay was used to acquire all ^{13}C NMR spectra, which were referenced to TMS ($\delta = 0$) by setting the high-frequency peak of a solid adamantane sample to 38.56 ppm.⁴⁷ ^1H MAS NMR spectra were acquired with a Bloch decay using a $4.0 \mu\text{s}$ 90°

^1H pulse, a 60 s recycle delay and a spinning frequency of 10 kHz. These were referenced to TMS ($\delta = 0$) by setting the residual ^1H peak of D_2O (99.9 % ^2H) to 1.80 ppm.

Isotropic chemical shifts (δ_{iso}) for the ^1H and ^{13}C spectra are assigned based on a visual inspection of the relevant spectra. The complex interactions leading to broad peaks in the ^{207}Pb NMR spectra precluded obtaining spectra of MAS samples and thus the isotropic chemical shift is not as clearly defined. We therefore report a chemical shift value (δ) that is the center-of-mass of the powder pattern. This value is expected to be close to the isotropic value. The center-of-mass was determined by fits of the powder pattern using WSOLIDS.⁴⁸ This program was also used to quantify contributions from various products to the NMR spectra, but the non-standard line shape for some spectra meant that this method was approximate.

2.5) Relative Humidity Control

The humidity experiments were conducted in a humidity-controlled, homebuilt flow cell (see Figure S1 in SI); the RH was measured continuously through a sensor placed inside the cell, which was placed in the dark. Reported RH values are accurate to within $\pm 5\%$. In humidity-only experiments, the temperature inside the cell was maintained at room temperature (293 ± 1 K). The humidity control technique is that reported previously;⁴⁹ to ensure that no liquid water entered the flow cell, an additional empty flask was added between the humidity source and the cell to serve as a water trap (Figure S1). In mixed humidity-heat experiments, a hot plate was placed inside the cell at a fixed temperature. In all experiments, the perovskite was ground using an agate mortar and pestle to a fine powder (~ 50 micron grains) and spread into an even thin layer in a borosilicate glass (Pyrex) petri dish within the cell. The cell was only opened to collect the samples after specific time points; the humidity within the cell returned quickly to the desired value (< 20 minutes after opening it).

3.) Results and Discussion

3.1) NMR Spectra of MAPbI₃ and Related Products

To investigate MAPbI₃ and proposed decomposition products resulting from its exposure to varying potential atmospheric conditions, ²⁰⁷Pb NMR spectra of stationary samples of MAPbI₃, MAPbI₃·H₂O (i.e., the monohydrate), (MA)₄PbI₆·2H₂O (i.e., the dihydrate) and PbI₂ were acquired, as shown in Figure 1. These spectra are notable for the distinct chemical shifts of the starting compound and its possible decomposition products. The range of isotropic chemical shifts (in excess of 1,400 ppm, see Table 1) is a reflection of the sensitivity of the ²⁰⁷Pb nucleus to its local environment and demonstrates the utility of NMR to characterize these types of materials. Chemical shifts and other NMR parameters derived from these spectra are summarized in Table 1. Dybowski and coworkers⁵⁰ reported a similar chemical shift value for PbI₂; values of 1430 and 1423 ppm were recently reported for MAPbI₃ by Roiland et al.⁵¹ and by Vela and coworkers,⁵² respectively. The slight difference in these chemical shift values compared to our value is probably a reflection of the extreme sensitivity of ²⁰⁷Pb to temperature.

Table 1. Solid-State NMR Parameters.

Sample	²⁰⁷ Pb		¹³ C	¹ H	
	δ/ppm	T ₁ /s ^a	δ/ppm	δ(NH ₃)/ppm	δ(CH ₃)/ppm
MAPbI ₃	1385(5)	1.16 ^b	31.3(1)	6.3(1)	3.2(1)
Monohydrate	485(50)	3.05(45)	27.5(3)	6.7(5)	2.6(1)
Dihydrate	375(10)	0.35(14)	30.9(4)	6.0(3)	3.2(2)
PbI ₂	-27(8)	1.20(10)	–	–	–
MAI	–	–	29.4(2)	6.5(5)	3.5(8)

a. Uncertainties assigned based on the 95 % confidence interval obtained from a three-parameter fit of the inversion recovery data.

b. Measured at 21.14 T at 335 K (i.e., the cubic phase).⁵³

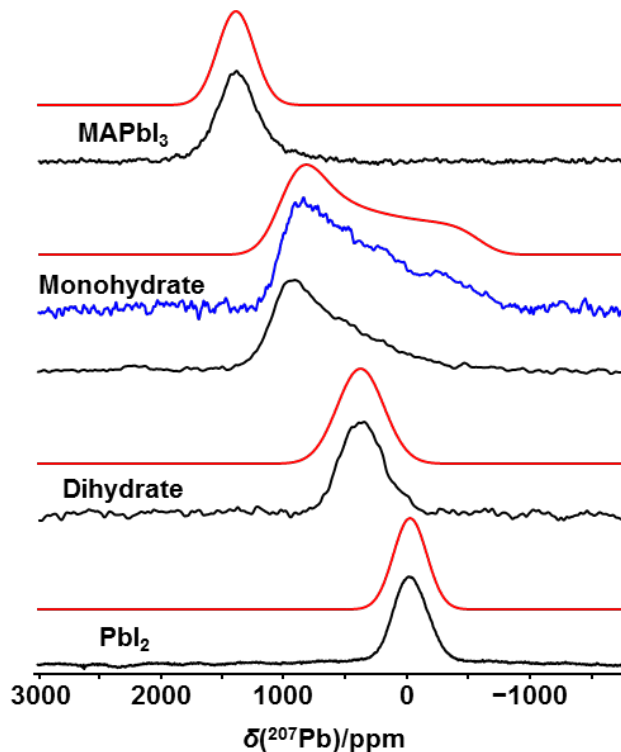


Figure 1. Simulated (red traces) and experimental ^{207}Pb NMR spectra of non-spinning samples of MAPbI_3 , the monohydrate, the dihydrate and PbI_2 , acquired at 294 K at 7.05 T. The blue trace indicates the skyline projection of experimental spectra for the monohydrate acquired with three spectrometer frequency offsets; all other spectra were acquired with a single frequency offset.

The ^{207}Pb NMR spectra for all samples considered here consist of broad powder patterns; those for MAPbI_3 , the dihydrate and for PbI_2 acquired at 7.05 T (Figure 1) are symmetric peaks with the full width at half maximum (FWHM) ranging from 20 to 27 kHz, while that for the monohydrate is an asymmetric peak whose breadth at the base spans approximately 120 kHz. Broad ^{207}Pb powder NMR line shapes have been reported previously for MAPbI_3 ^{51, 52} and for PbI_2 ⁵⁰. The broadening must be due to properties of the material rather than due to instrumental or environmental factors, since ^{207}Pb NMR spectra for the setup compound ($\text{Pb}(\text{NO}_3)_2$) had the expected sharp peaks under MAS conditions. For a $I=1/2$ nucleus like Pb-207 possible causes include (i) magnetic shielding anisotropy, (ii) a dispersion of chemical shift values due to molecular disorder, (iii) direct dipolar coupling, R_{DD} , to neighboring spin-active nuclei, (iv) indirect spin-spin coupling $^1J(^{207}\text{Pb}, ^{127}\text{I})$,^{50, 53} or (v) most likely a combination of these contributions. The simulated spectra shown in Figure 1 were

obtained with the assumption of no anisotropic magnetic shielding for MAPbI₃, the dihydrate or PbI₂, but with a span ($\delta_{11} - \delta_{33}$) of more than 1500 ppm, shielding is present for the monohydrate. However, given the broad powder patterns observed here, magnetic shielding anisotropy cannot be excluded for any of these compounds. Note that each Pb nucleus is coordinated to six ¹²⁷I nuclei ($I = 5/2$, natural abundance = 100 %) so that even modest direct or indirect spin-spin interactions would lead to significant broadening of the ²⁰⁷Pb NMR peaks. Dybowski and coworkers have provided a detailed discussion of factors affecting the line width for the ²⁰⁷Pb NMR spectra of PbI₂.⁵⁰

To ensure quantitative data when more than one NMR site is observed, the ²⁰⁷Pb spin-lattice relaxation times (i.e., T_1 values) were measured for MAPbI₃ and its related products, using a modified inversion-recovery pulse sequence (see Experimental Section). These values, which range from 0.35 to 3.05 s, are also listed in Table 1. That for MAPbI₃ was measured at 335 K (i.e., the cubic phase), but was reported to be much shorter (50 ms) by Roiland et al.⁵¹ at room temperature, when the compound is in the tetragonal phase.^{54, 55}

Figure 2 illustrates ¹³C and ¹H MAS NMR spectra of the samples; see Table 1 for a summary of the ¹³C and ¹H chemical shifts. The unusually sharp peaks and limited number of spinning sidebands for the ¹H NMR spectrum of MAPbI₃ reflect the high mobility of the MA⁺ ion in this complex,⁵⁶ which lead to significant reduction in the effective dipolar coupling between ¹H nuclei. The bulk of the ¹H NMR signal for the monohydrate is distributed over a broad spinning sideband pattern, but this is somewhat obscured by a very sharp peak, attributed to mobile surface H₂O (see Fig. 2, inset), whose intensity is a small percentage of the total intensity for this spectrum; rapid dehydration of the monohydrate to MAPbI₃ (below) made it difficult to obtain a perfectly dry sample of the former. As seen when the vertical scale is multiplied, there is a broad underlying spinning sideband pattern, attributed to the ¹H nuclei for the MA⁺ cation; the breadth of these peaks indicates

restricted motion of MA⁺ in this case. Likewise, similar spinning sideband patterns for the dihydrate and for MAI indicate restricted motion for MA⁺ in these cases. Although the ¹³C isotropic chemical shifts fall within a narrow range (~ 4 ppm), the resolution obtained with MAS is such that ¹³C NMR spectra can be used to identify if a decomposition product is the monohydrate or MAI.

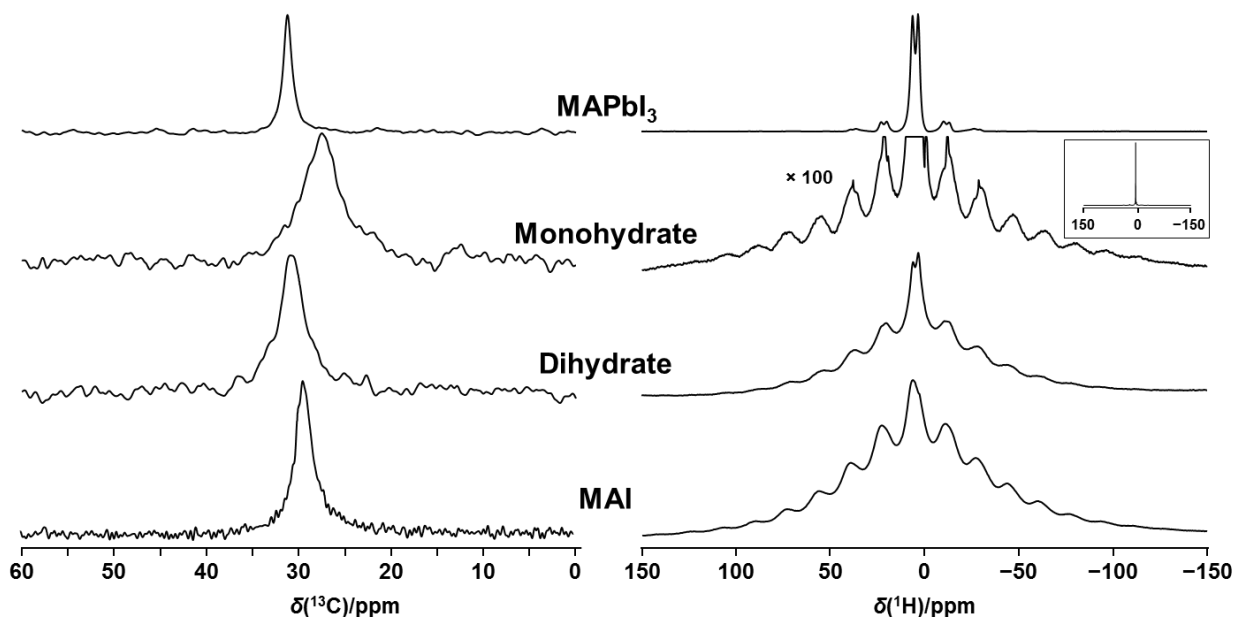


Figure 2. ¹³C (left) and ¹H (right) MAS NMR spectra for MAPbI₃, the monohydrate and dihydrate samples and for MAI. All ¹³C NMR spectra were acquired with CP at 7.05 T at a spinning frequency of 5 kHz. All ¹H NMR spectra were acquired with a Bloch decay pulse sequence at a spinning frequency of 5 kHz, at 7.05 T. The inset shows the complete ¹H NMR spectrum for the monohydrate, which is dominated on the vertical scale by a sharp peak attributed to surface H₂O.

3.2) Powder X-Ray Diffraction

Figure 3 shows experimental XRD patterns obtained in this work. The simulations, based on the reported structures for MAPbI₃,⁵⁷ PbI₂ (PDF 00-007-0235), the monohydrate⁵⁸ or the dihydrate,⁵⁹ confirm that the desired products have been obtained. As for the ²⁰⁷Pb NMR spectra, distinctive powder XRD patterns are obtained for the four compounds. Table S1 summarizes the structural parameters obtained from the reported single-crystal X-ray studies. The latter suggest that each are expected to have a single ²⁰⁷Pb site although only the ²⁰⁷Pb nuclei of PbI₂ are at sites of octahedral

symmetry, so the other compounds may yield anisotropic magnetic shielding powder patterns (e.g., the monohydrate). Single ^{13}C NMR sites and two distinct ^1H sites from the MA cations are expected for MAPbI_3 as well as the monohydrate and the dihydrate.

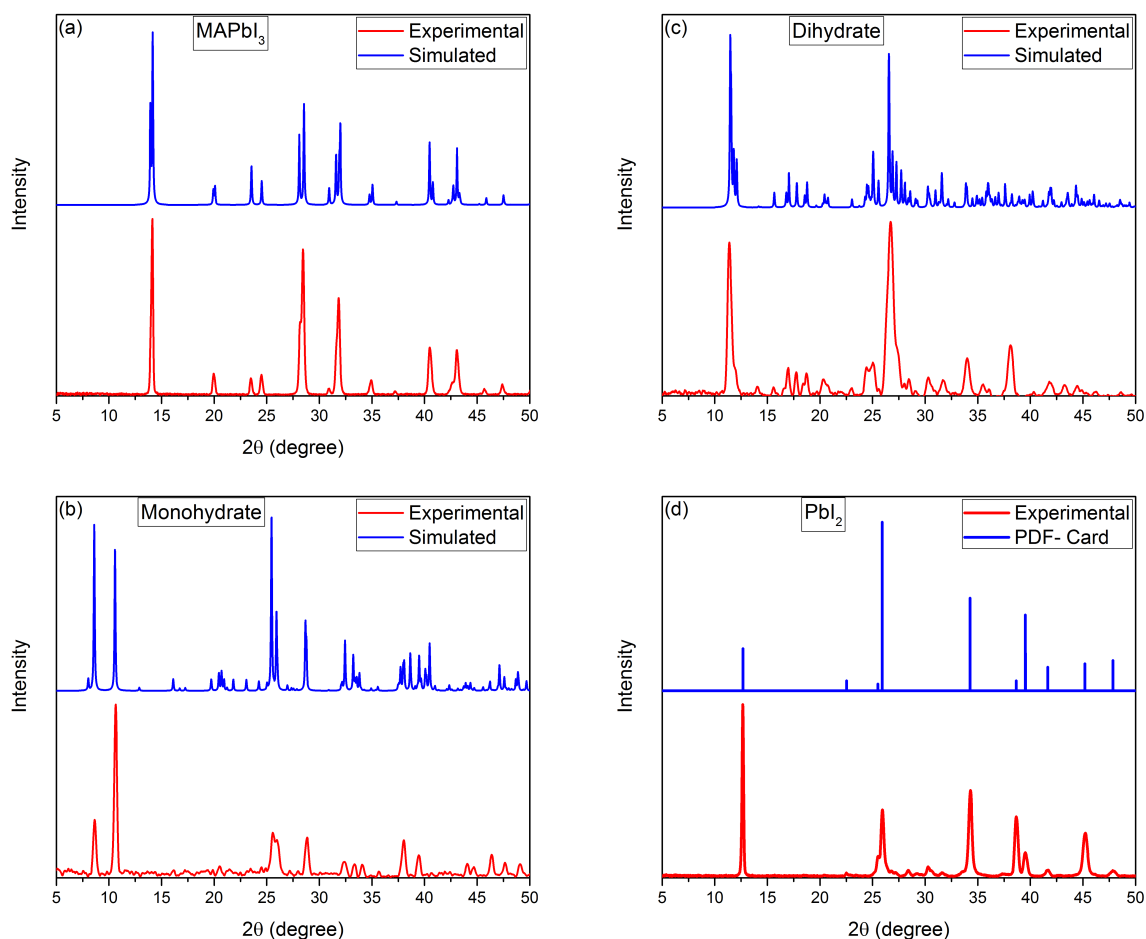


Figure 3. Experimental and simulated powder X-ray diffraction patterns for crystalline MAPbI_3 (a), the monohydrate (b), the dihydrate (c), and PbI_2 (d).

3.3) Response of MAPbI_3 to Humidity at Ambient Temperature

To investigate the effect of humidity on MAPbI_3 , approximately 1.0 g of the sample was placed in a humidifier operating at room temperature, at approximately 80 % RH. In the course of one week, the sample turned from the black color of MAPbI_3 to a yellow crystalline powder (see Figure S1). Figure 4 illustrates ^{207}Pb NMR spectra of stationary samples extracted from the humidifier at the indicated times, ranging from 3 hours to 3 weeks; a spectrum of MAPbI_3 (i.e., $t = 0$)

is included for comparison. These spectra demonstrate that MAPbI₃ is quickly affected by humidity; approximately 55 % of the total signal has shifted to an asymmetric peak after exposure to 80 % RH for three hours. After 24 hours, this peak had grown to 80 % of the total intensity, after three days only a trace of the peak attributed to MAPbI₃ remained, and finally, after one week, only the asymmetric peak remained. As seen from the spectrum of the sample collected after 21 days, there were no further changes once the product yielding the asymmetric peak was obtained. Comparison of the ²⁰⁷Pb NMR spectra shown in the upper traces of Figure 4 with those shown in Fig. 1 along with the ¹³C NMR spectra (Figure 2 and S2) indicate that the product of exposure of MAPbI₃ to high humidity is the monohydrate, with no indication that any further decomposition occurs. A powder XRD pattern obtained for the *t* = 21 day sample, simulated using the single-crystal XRD data for the monohydrate (see Figure S3),⁵⁸ confirms that the product is the monohydrate; as for the ²⁰⁷Pb spectra, there is no indication from this XRD pattern that either the dihydrate or of PbI₂ are decomposition products.

Figure S2 shows ¹³C and ¹H MAS NMR spectra of MAPbI₃ exposed to humidity. The formation of the monohydrate is clearly established, since it has a distinct ¹³C chemical shift; intensity ratios for a given exposure period vary from the corresponding ²⁰⁷Pb NMR spectrum, reflecting the non-quantitative nature of the CP technique used to acquire the ¹³C spectra. A small peak at 31.2 ppm seen in the *t* = 7 days ¹³C spectrum is attributed to residual MAPbI₃ rather than the onset of the formation of the dihydrate, which has the same chemical shift (see Table 1) since by 21 days that peak is no longer seen; such a low intensity contribution would not be detected in the ²⁰⁷Pb spectrum. There is no indication from the ¹³C spectra that MAI is a significant decomposition product; this is expected since the formation of MAI would require the concurrent formation of PbI₂, which is not indicated from the ²⁰⁷Pb NMR spectra shown in Figure 4.

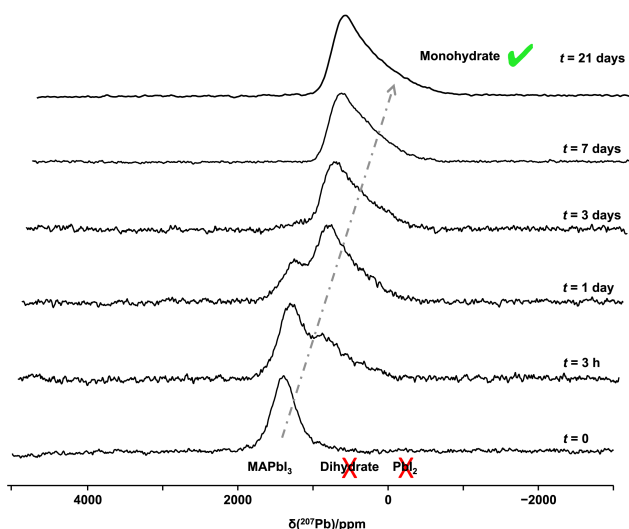


Figure 4. ^{207}Pb NMR spectra of stationary samples acquired at the indicated times after the start of humidification at 80 % at 293 ± 1 K. Spectra were acquired at 7.05 T.

The response of the monohydrate to elevated temperatures was investigated *via* NMR spectroscopy. Figure 5 illustrates ^{207}Pb NMR spectra of a stationary sample of the monohydrate acquired in the 293 to 341 K temperature range. Because of possible dehydration during the two-hour time period needed to acquire the individual spectra shown in this figure, subspectra were acquired in 30-minute time blocks under identical conditions and the resulting free induction decays were summed prior to processing. There was no variation in the subspectra acquired for a given temperature up to and including 313 K, indicating that dehydration did not occur at or below this temperature. However, as seen in Figure S4, at 324 K the intensity of the peak attributed to the monohydrate diminished significantly in the course of the two hours required to acquire the total spectrum, suggesting dehydration of the monohydrate. The peak at 1380 ppm arising from MAPbI_3 was not immediately detected, although, as seen in Figure 5, it was observed for a spectrum acquired at 341 K. The lower sensitivity of the ^{207}Pb NMR signal from MAPbI_3 was observed for other spectra in this work and is thought to be a consequence of a shorter T_2 relaxation time for MAPbI_3 at this temperature (the compound undergoes a phase transition from tetragonal to cubic at 326.6 K);⁵⁴,⁵⁵ acquisition of ^{207}Pb NMR spectra in the 1000 to 2000 ppm range at 11.75 T (our only option for

non-ambient temperature measurements) is further complicated by interference from a local radio station. Nevertheless, spectra shown in Fig. 5 clearly indicate that MAPbI₃ can indeed be recovered from the monohydrate with moderate heating. To further verify that MAPbI₃ had been recovered, ¹H, ¹³C and ²⁰⁷Pb NMR spectra of the sample were acquired at 7.05 T (see Figure S5 in SI). These spectra are virtually identical to those for MAPbI₃, also shown in this figure.

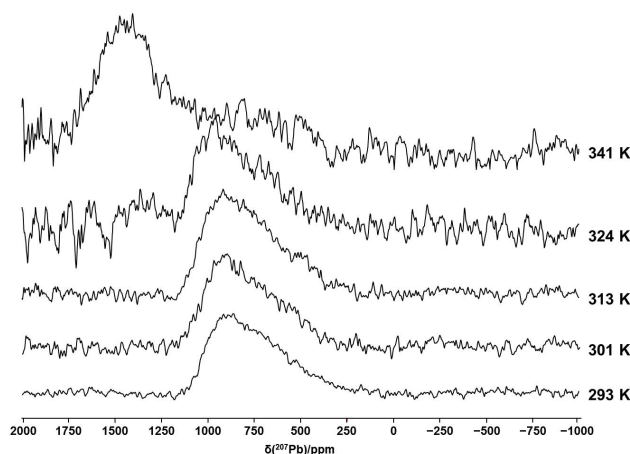


Figure 5. ²⁰⁷Pb NMR spectra of a stationary sample of MAPbI₃·H₂O acquired at 11.75 T at the indicated temperatures. Each spectrum shown here is the sum of four sub-spectra acquired under the same conditions. The spectrum acquired at 324 K is noisier because of dehydration of the monohydrate (see text).

When the monohydrate was first synthesized according to literature methods, it dehydrated under ambient conditions in a period of minutes, turning from yellow to black if exposed to air, unless stored in a sealed container. However, in the course of our investigations, we observed that the monohydrate obtained by placing a finely ground MAPbI₃ sample in the humidifier at 80 % RH for a long period of time (three weeks) did not dehydrate as rapidly. To investigate, the sample was exposed to the atmosphere by leaving it in an open beaker for over four hours. There was no indication of dehumidification (i.e., the sample remained yellow rather than turning black). However, when placed in an oven at 373 K, the sample turned black in less than thirty minutes, indicating that MAPbI₃ had been recovered. The XRD pattern for this three-week sample obtained prior to exposure

to the atmosphere or to high temperatures, shown in Figure S3, indicates high crystallinity, which may explain why it is more stable and less vulnerable to dehydration.

Several of the preceding observations on the response of bulk MAPbI₃ to high relative humidity has also been reported for the sample on films. Berger and coworkers,²¹ Leguy et al.¹³ and Zhao et al.⁶⁰ reported the formation of the monohydrate following exposure of MAPbI₃ films to 80 % relative humidity, while Yang et al. described the product of humidification as the dihydrate “or a very closely related hydrate”.²⁴ These groups all reported that MAPbI₃ could be recovered from the monohydrate. However, contrary to our observations, Berger and coworkers found that long-term (i.e., > 6 days) exposure of the film to RH = 80 % lead to the formation of the dihydrate and also detected the presence of PbI₂,²¹ as did Zhao et al.⁶⁰ who also reported the formation of MAI (vide infra). Likewise, Leguy et al.¹³ reported the dihydrate as a decomposition product of high humidity, but only traces of PbI₂ were detected despite predictions based on Equation 2. The latter authors speculate that PbI₂ may be in an amorphous or nanocrystalline phase and thus difficult to detect *via* XRD.

The sensitivity of MAPbI₃ to high RH leads one to question whether the sample is also sensitive to lower RH levels. To investigate, a sample of MAPbI₃ was placed in the humidifier in a 40 % RH environment at 293 K for 11 days. The compound remained black and its ¹H, ¹³C and ²⁰⁷Pb NMR spectra (Figure S6) were very similar to those for MAPbI₃, indicating that bulk MAPbI₃ is stable at this level of humidity. This is similar to the observations of Wang and Chen,⁶¹ who found that at 40% RH a MAPbI₃ solar cell (with no capsulation) remained mostly unchanged for 100 days, with no evidence of the decomposition of the MAPbI₃ to a hydrate or to PbI₂. These authors reported that the stability of MAPbI₃ depends greatly on the purity and morphology of the film. Berger and coworkers²¹ also found that MAPbI₃ is unaffected for RH ≤ 50 %. In contrast, Shirayama and coworkers²⁷ recently investigated thin layers of MAPbI₃ on film, prepared by a laser evaporation

technique, and found that at 40% RH, the sample degraded in one day through the formation of both PbI_2 and the dihydrate.

3.3) Response of MAPbI_3 to Direct Exposure to $\text{H}_2\text{O}(\text{l})$ at Ambient Temperature

In their investigation of MAPbI_3 , Leguy et al.¹³ reported that exposure to $\text{H}_2\text{O}(\text{l})$ led to the irreversible formation of PbI_2 ; intermediate products (i.e., the monohydrate or the dihydrate) were not observed. These authors undertook their measurements on thin films. To determine whether the same holds true for the fine powders investigated in this work, 50 μL $\text{H}_2\text{O}(\text{l})$ was added to approximately 200 mg of MAPbI_3 . Comparison of the ^{207}Pb NMR spectra before and after addition of the H_2O (Figures 6a and 6b, respectively) demonstrates that the monohydrate is obtained under these conditions, contrary to the observations of Leguy et al.¹³ Considering the low stability of the monohydrate, the sample was packed into an NMR rotor immediately following the addition of $\text{H}_2\text{O}(\text{l})$. Following the acquisition of the spectrum shown in Fig. 6b, the sample was removed from the rotor and placed in a petri dish to which a further 200 μL $\text{H}_2\text{O}(\text{l})$ was added. To ensure that the sample was dry, it was allowed to stand overnight under ambient conditions before it was packed; the spectrum obtained from this sample, which shows that PbI_2 is indeed obtained after exposure to a sufficient amount of $\text{H}_2\text{O}(\text{l})$, is shown in Figure 6c. To verify that the peak at -27 ppm is not due to a previously undetected hydration product, the sample was then placed in a petri dish and dried for three hours at 343 K (above the MAPbI_3 tetragonal-cubic phase transition). The spectrum, shown in Fig. 6d, is unchanged, consistent with the formation of PbI_2 . The ratio of MAPbI_3 : PbI_2 is approximately 2:1, although this value is no doubt dependent on initial conditions. Note that the ease with which the monohydrate was initially formed and its rapid dehydration suggest that it is almost certainly an intermediate product between MAPbI_3 and PbI_2 such that, depending on how soon after exposure to $\text{H}_2\text{O}(\text{l})$ the spectrum is acquired, a spectrum with contributions from only the monohydrate and PbI_2 , or one with contributions from all three compounds might be obtained.

However, we saw no evidence for the dihydrate in this series of measurements. Considering Equations 1 and 2, MAI is expected as a decomposition product along with PbI_2 , with a 2:1 ratio of ^{13}C intensity from the MAPbI_3 and MAI. From Figure S7, the ^{13}C peak for MAI is not detected, but given the much greater linewidth expected for the MAI ^{13}C and the non-quantitative nature of the CP technique used to acquire this spectrum, the presence of any signal may be lost in the noise. Indeed, although the ^1H spectrum is dominated by the peaks attributed to MAPbI_3 , the vertical expansion of this spectrum (Figure S7) indicates the broad spinning sideband pattern expected from MAI.

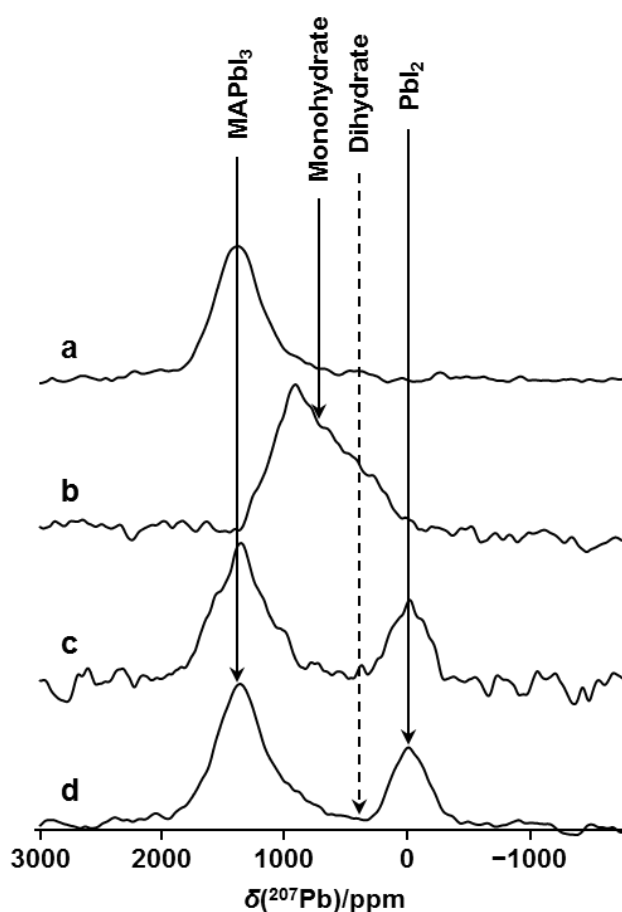


Figure 6. Stationary ^{207}Pb NMR spectra of (a) MAPbI_3 , (b) the sample from (a) following the addition of 50 μL H_2O , (c) the sample from (b) following the addition of a further 200 μL H_2O and (d) the spectrum from (c) after it was heated at 343 K for three hours. The solid lines indicate the chemical shifts of identified compounds, while the dotted line is that for a proposed decomposition product that was not observed. Spectra were acquired at 7.05 T and 294 K.

3.4) Response of MAPbI_3 to Humidity at Elevated Temperatures

Understanding the response of MAPbI₃ to elevated temperatures is an important consideration if it is to be used in solar cells, since the absorbed light energy elevates the temperature of the apparatus to above 350 K.²⁸ In fact, damp-heat testing is an important component of commercial solar panel design.²⁴ Although MAPbI₃ transitions from the tetragonal to the cubic phase at 326.6 K,^{54, 55, 62} there is no significant chemical shift effect due to this transition.⁵³ Thus significant changes to the ²⁰⁷Pb NMR chemical shifts at elevated temperatures indicate a response to environmental conditions, rather than merely being a consequence of the phase transition. To investigate the response of MAPbI₃ to elevated temperatures and humidity, a powder sample was placed in a petri dish on a hot plate inside a humidity-controlled cell with the temperature of the hot plate maintained at 358 ± 3 K and the humidity of the cell maintained at 45 ± 5 %. The presence of the hot plate within the cell increased the surrounding air temperature to 308 ± 2 K. Samples were extracted after 0, 3, and 24 hours, as well as 8 days. The sample was sealed within a zirconia NMR rotor immediately after extraction from the humidifier, although it was not always possible to immediately acquire the NMR spectra; there was no indication that the sample degraded over time once packed. Figure 7 illustrates the ²⁰⁷Pb NMR spectra of these samples. After three hours, decomposition products, if present, are not detected. However, after 24 hours, a ²⁰⁷Pb NMR peak at the position expected for PbI₂ is detected; this peak contributes approximately 30 % of the total intensity. The process of decomposition under these conditions proceeds at a slow pace; after 8 days, PbI₂ contributes approximately 55 % of the total NMR signal. The process is expected to continue until only PbI₂ remains, although this would take several weeks under the conditions described here. If any monohydrate or dihydrate was produced during this process, their ²⁰⁷Pb NMR signal was of insufficient intensity to be detected. In their investigation of encapsulated MAPbI₃ solar cells, Han et al.²⁸ also found that PbI₂ was a decomposition product of the sample placed under conditions of heat and humidity, though in this case, the Ag layer forming part of the solar cell may have been a factor.

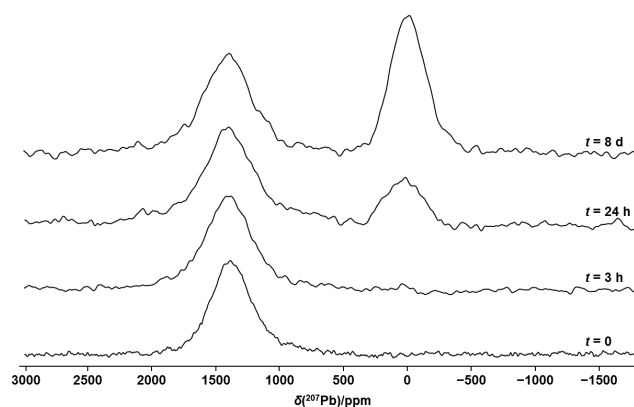


Figure 7. ^{207}Pb NMR spectra of stationary samples of MAPbI_3 (1385 ppm) and its product PbI_2 (-27 ppm) following exposure to heat (358 K) and 45 % RH. Spectra were acquired at 293 K at 7.05 T.

Zhao et al.⁶⁰ found that the final degradation products of treatment of MAPbI_3 (deposited on tin oxide glass) to high humidity and heat was PbI_2 and $\text{MAI}(\text{aq})$ and that the latter did not decompose further to MA and HI. If MAI persisted, its presence would be detectable by ^1H and ^{13}C NMR spectroscopy. The ^1H and ^{13}C NMR spectra for the sample after it was subjected to eight days of heat and humidity are compared with those for MAI and MAPbI_3 in Figure S8. Based on the ^{207}Pb NMR spectra for this sample (Figure 7), the contribution from MAI should be approximately 55 %; despite the broader ^1H and ^{13}C NMR peaks from MAI, such a percentage would be detected. Since there is no indication that MAI persists as a decomposition product when considering the bulk sample, it is assumed to have escaped as $\text{CH}_3\text{CH}_2(\text{g}) + \text{HI}(\text{g})$. MAI was detected on the other occasion where PbI_2 was detected in this work, when MAPbI_3 was exposed to an excess of $\text{H}_2\text{O}(\text{l})$ at room temperature (vide supra). Clearly, the evolution of MAI is also sensitive to environmental conditions.

This series of measurements demonstrates that under moderately elevated temperatures and a humid environment, MAPbI_3 slowly decomposes to PbI_2 . The process is slow, but since it is irreversible, it is a serious concern for solar cell engineers.

3.5) Response of MAPbI₃ to Elevated Temperatures

To ascertain that both heat and humidity are required to drive the decomposition of MAPbI₃ to PbI₂, we also studied the effect of exposing MAPbI₃ to an elevated temperature in a dry environment. A fine MAPbI₃ powder sample was placed in a furnace at 378 K for 4 days, then packed into an NMR rotor immediately after removal from the furnace. Comparison of the ¹H, ¹³C and ²⁰⁷Pb NMR spectra of the product with those for MAPbI₃ (see Figure S9 in SI) indicates that the product remains MAPbI₃, with no indication of PbI₂ or MAI. In their study of encapsulated MAPbI₃ solar cells discussed above, Han et al.²⁸ did find some degradation of the solar cell performance when exposed to elevated temperatures and low (10 %) humidity, although the degradation was not as extreme as when both heat and humidity were present.

3.6) Response of the Dihydrate to Elevated Temperatures

The dihydrate has been proposed as the second step in the decomposition of MAPbI₃ to PbI₂ (Equation 1),¹³ and as for the monohydrate, this step is thought to be reversible. Hence ²⁰⁷Pb NMR spectra of a stationary dihydrate sample, prepared as outlined above, were acquired at elevated temperatures to determine if MAPbI₃ can be recovered from the dihydrate and whether the monohydrate is an intermediate step in this recovery. Spectra (not shown) acquired at 301 and 313 K were virtually identical to that for the dihydrate shown in Figure 1. Obtaining these ²⁰⁷Pb NMR spectra was hampered by the limited sample volume (approximately 85 mg, or 1/3 of the 4 mm NMR rotor), by the fact that following the onset of dehydration, it proceeds quickly, and by the difficulties in obtaining variable temperature NMR data as discussed above; thus the spectra we obtained had a low signal/noise ratio. Nevertheless, as seen in Figure 8, we are able to follow the dehydration process via ²⁰⁷Pb NMR spectroscopy. A spectrum acquired at 324 K (Figure 8a) is virtually identical to that obtained for the dihydrate at room temperature (Figure 1). However, by the time the next

spectrum was acquired, approximately 15 minutes after the temperature had stabilized at 336 K, a broad peak, covering the frequency range seen for the monohydrate and the dihydrate, was observed (Figure 8b; a comparison with those for the monohydrate and dihydrate is shown in the inset), suggesting that part of the sample was dehydrating such that the monohydrate was obtained. During acquisition of the four subsequent spectra (Figures 8c to 8f), each of which took 15 minutes, first the signal at the position of the dihydrate was lost, and by the last spectrum, virtually all the signal attributed to the monohydrate was also lost. The loss of the signal attributed to the monohydrate is unsurprising since it was also lost when the monohydrate was heated at 324 K (see Figure S4). As discussed above, detecting MAPbI_3 at 11.75 T proved challenging. Nevertheless, a spectrum obtained the following day at 7.05 T (Figure 8g) confirmed that MAPbI_3 had been recovered.

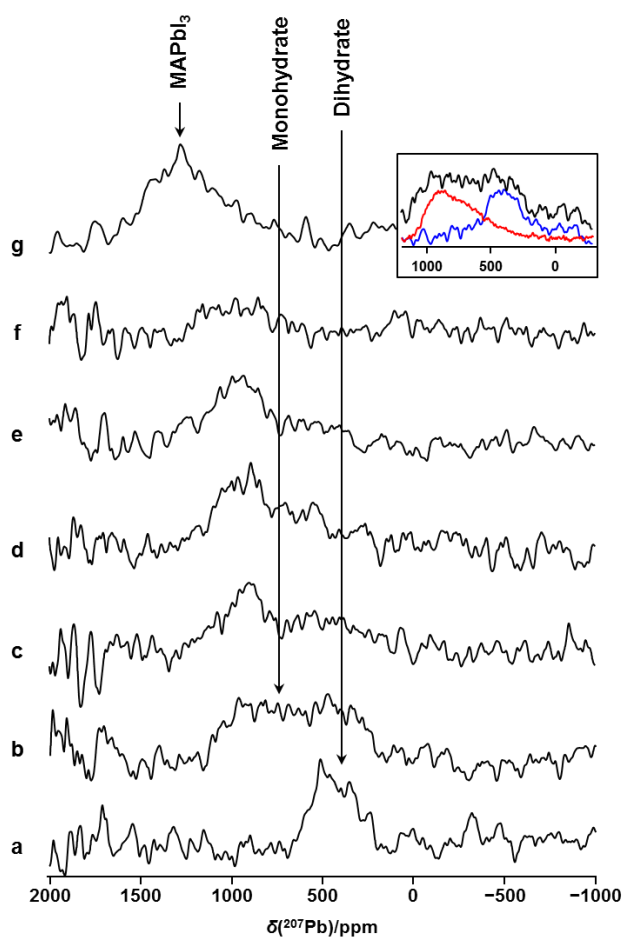


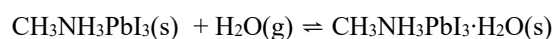
Figure 8. Stationary ^{207}Pb NMR spectra illustrating the response of the dihydrate³⁹ to elevated temperatures. (a): a spectrum acquired at 324 K; (b-f): a series of spectra acquired at 336 K in 15

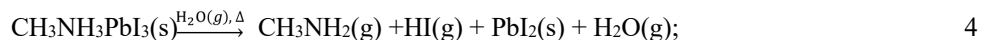
minute increments. These spectra are of stationary samples, acquired at 11.75 T; the noise to high frequency is attributed to interference from a local FM radio station. In (g), a spectrum of the stationary sample acquired on the following day at 7.05 T at 294 K is shown. In the inset, the spectrum shown in (b) is compared to those for the monohydrate (red) and the dihydrate (blue).

The dihydrate was not observed in any of our experiments as a degradation product of MAPbI₃, which is not surprising since, to the best of our knowledge, the only way to prepare the pure dihydrate requires an excess of the MAI, which is how the sample used here was synthesized.³⁹ Starting with pure MAPbI₃ with a 1:1 molar ratio of MAI: PbI₂, it is unlikely that the dihydrate would form.

4.0 Conclusions

We have presented a multinuclear solid-state NMR study of MAPbI₃ and of its proposed decomposition products: the monohydrate and dihydrate derivatives of the compounds, as well as PbI₂. We have demonstrated that ²⁰⁷Pb NMR is a sensitive technique to distinguish which of these products, if any, have been obtained. Although more ambiguous, ¹H and ¹³C NMR spectroscopy can also inform on this problem. A significant conclusion of our investigations is that exposure of bulk samples of MAPbI₃ to high humidity under ambient temperature conditions leads to the formation of the monohydrate but not to other decomposition products. This is in contrast to many studies of MAPbI₃ on films; since the MAPbI₃ is easily recovered from the monohydrate, this is an important observation. However, exposure to both heat and humidity, or to excess H₂O(l), does lead to an irreversible decomposition, with PbI₂ as the main solid product. The varying observations discussed in this section and summarized in Table 2 and Scheme 1 demonstrate the high-sensitivity of MAPbI₃ to subtle differences in conditions or in the preparation of the sample. Based on our observations, Equations 3, 4 and 5 are proposed to describe the sensitivity of MAPbI₃ to heat, or humidity or water:





In the work discussed here, heat was used to recover MAPbI₃ from the monohydrate. However, the monohydrate dehydrates spontaneously under ambient conditions, albeit slowly if we are dealing with samples that were annealed within the humidifying chamber over prolonged periods of time. The XRD and NMR data (Figures S3 and S10) suggest that increases the degree of crystallinity; the diffraction peaks and ¹³C resonance narrow considerably for the finely ground samples discussed above.

Table 2: Summary of MAPbI₃ degradation products under humidity and thermal treatments

Products	MAPbI ₃	Monohydrate	Dihydrate	PbI ₂
I	X	X		
II	X			
III	X	X		
IV		X		
V	X			X
VI	X			X
VII	X	X	X	
VIII	X			X
IX	X			

- I. MAPbI₃ placed in a humidity chamber at 80% RH over a period of up to 21 days at 293 K.
- II. MAPbI₃ – Cycling between tetragonal and cubic phase of MAPbI₃ (*in situ* NMR)
- III. Monohydrate from **I** (*t* = 7 days) heated to 341 K, then back to 293 K; i.e., the monohydrate dehydrated back to MAPbI₃ (*in situ* NMR)
- IV. 50 μL H₂O(l) added to MAPbI₃
- V. 200 μL added to the product of **IV**; sample allowed to dry under ambient conditions overnight
- VI. Sample from **V**, placed in a furnace at 343 K for 4 hours
- VII. The synthesized dihydrate, heated through the tetragonal and cubic phase transition for MAPbI₃, forming the monohydrate, then MAPbI₃ (*in situ* NMR)
- VIII. MAPbI₃ placed on a hot plate at 358 K and 45 % humidity
- IX. MAPbI₃ placed in an oven at 378 K for 4 days, then packed in an NMR rotor and spectra acquired at room temperature

Sample stability is a critical consideration for solar cell engineers. Our study suggests that the bulk material is much more stable than thin films. We hope that information provided here may serve as a guide in ongoing efforts to understand the intrinsic stability of MAPbI₃ and its use in the design

and fabrication of these promising commercial hybrid organic-inorganic perovskite solar cell materials.

Supporting Information:

Supporting Information is available online or from the author. Flow cell images; additional ^1H , ^{13}C , ^{207}Pb NMR spectra; XRD experimental and simulated powder patterns.

Acknowledgements:

The Natural Sciences and Engineering Research Council (NSERC) of Canada and the University of Alberta are acknowledged for generous support of this research (VKM). AMA acknowledges scholarship support from Alberta Innovates Technology Futures (AITF). KS acknowledges direct and indirect (equipment) funding support from NRC-NINT and CFI. The authors thank Prof. Wasylishen for valuable scientific discussions and Mr. D. Starke (Chemistry, University of Alberta) for constructing the humidifying flow cell.

References:

1. Kojima, A.; Teshima, K.; Shirai, Y.; Miyasaka, T., Organometal Halide Perovskites as Visible-Light Sensitizers for Photovoltaic Cells. *Journal of the American Chemical Society* **2009**, *131*, 6050-6051.
2. Saliba, M.; Matsui, T.; Seo, J.-Y.; Domanski, K.; Correa-Baena, J.-P.; Nazeeruddin, M. K.; Zakeeruddin, S. M.; Tress, W.; Abate, A.; Hagfeldt, A., *et al.*, Cesium-Containing Triple Cation Perovskite Solar Cells: Improved Stability, Reproducibility and High Efficiency. *Energy & Environmental Science* **2016**, *9*, 1989-1997.
3. Li, X.; Bi, D.; Yi, C.; Décoppet, J.-D.; Luo, J.; Zakeeruddin, S. M.; Hagfeldt, A.; Grätzel, M., A Vacuum Flash-Assisted Solution Process for High-Efficiency Large-Area Perovskite Solar Cells. *Science* **2016**, *353*, 58-62.
4. Bi, D.; Tress, W.; Dar, M. I.; Gao, P.; Luo, J.; Renevier, C.; Schenk, K.; Abate, A.; Giordano, F.; Correa Baena, J.-P., *et al.*, Efficient Luminescent Solar Cells Based on Tailored Mixed-Cation Perovskites. *Science Advances* **2016**, *2*, e1501170.
5. Yang, W. S.; Noh, J. H.; Jeon, N. J.; Kim, Y. C.; Ryu, S.; Seo, J.; Seok, S. I., High-Performance Photovoltaic Perovskite Layers Fabricated through Intramolecular Exchange. *Science* **2015**, *348*, 1234-1237.
6. Po, R.; Bianchi, G.; Carbonera, C.; Pellegrino, A., "All That Glisters Is Not Gold": An Analysis of the Synthetic Complexity of Efficient Polymer Donors for Polymer Solar Cells. *Macromolecules* **2015**, *48*, 453-461.
7. Bretschneider, S. A.; Weickert, J.; Dorman, J. A.; Schmidt-Mende, L., Research Update: Physical and Electrical Characteristics of Lead Halide Perovskites for Solar Cell Applications. *APL Mater.* **2014**, *2*, 040701.
8. Kazim, S.; Nazeeruddin, M. K.; Grätzel, M.; Ahmad, S., Perovskite as Light Harvester: A Game Changer in Photovoltaics. *Angewandte Chemie International Edition* **2014**, *53*, 2812-2824.
9. Xing, G.; Mathews, N.; Sun, S.; Lim, S. S.; Lam, Y. M.; Grätzel, M.; Mhaisalkar, S.; Sum, T. C., Long-Range Balanced Electron- and Hole-Transport Lengths in Organic-Inorganic $\text{CH}_3\text{NH}_3\text{PbI}_3$. *Science* **2013**, *342*, 344-347.
10. Stranks, S. D.; Eperon, G. E.; Grancini, G.; Menelaou, C.; Alcocer, M. J. P.; Leijtens, T.; Herz, L. M.; Petrozza, A.; Snaith, H. J., Electron-Hole Diffusion Lengths Exceeding 1 Micrometer in an Organometal Trihalide Perovskite Absorber. *Science* **2013**, *342*, 341-344.
11. Park, N.-G., Perovskite Solar Cells: An Emerging Photovoltaic Technology. *Materials Today* **2015**, *18*, 65-72.
12. Noh, J. H.; Im, S. H.; Heo, J. H.; Mandal, T. N.; Seok, S. I., Chemical Management for Colorful, Efficient, and Stable Inorganic–Organic Hybrid Nanostructured Solar Cells. *Nano Letters* **2013**, *13*, 1764-1769.
13. Leguy, A. M. A.; Hu, Y.; Campoy-Quiles, M.; Alonso, M. I.; Weber, O. J.; Azarhoosh, P.; van Schilfgaarde, M.; Weller, M. T.; Bein, T.; Nelson, J., *et al.*, Reversible Hydration of $\text{CH}_3\text{NH}_3\text{PbI}_3$ in Films, Single Crystals, and Solar Cells. *Chemistry of Materials* **2015**, *27*, 3397-3407.
14. Gangishetty, M. K.; Scott, R. W. J.; Kelly, T. L., Effect of Relative Humidity on Crystal Growth, Device Performance and Hysteresis in Planar Heterojunction Perovskite Solar Cells. *Nanoscale* **2016**, *8*, 6300-6307.
15. Gao, H.; Bao, C.; Li, F.; Yu, T.; Yang, J.; Zhu, W.; Zhou, X.; Fu, G.; Zou, Z., Nucleation and Crystal Growth of Organic–Inorganic Lead Halide Perovskites under Different Relative Humidity. *ACS Applied Materials & Interfaces* **2015**, *7*, 9110-9117.
16. You, J.; Yang, Y.; Hong, Z.; Song, T.-B.; Meng, L.; Liu, Y.; Jiang, C.; Zhou, H.; Chang, W.-H.; Li, G., *et al.*, Moisture Assisted Perovskite Film Growth for High Performance Solar Cells. *Applied Physics Letters* **2014**, *105*, 183902.
17. Zhou, H.; Chen, Q.; Li, G.; Luo, S.; Song, T.-b.; Duan, H.-S.; Hong, Z.; You, J.; Liu, Y.; Yang, Y., Interface Engineering of Highly Efficient Perovskite Solar Cells. *Science* **2014**, *345*, 542-546.
18. Berhe, T. A.; Su, W.-N.; Chen, C.-H.; Pan, C.-J.; Cheng, J.-H.; Chen, H.-M.; Tsai, M.-C.; Chen, L.-Y.; Dubale, A. A.; Hwang, B.-J., Organometal Halide Perovskite Solar Cells: Degradation and Stability. *Energy & Environmental Science* **2016**, *9*, 323-356.

19. Hu, L.; Shao, G.; Jiang, T.; Li, D.; Lv, X.; Wang, H.; Liu, X.; Song, H.; Tang, J.; Liu, H., Investigation of the Interaction between Perovskite Films with Moisture Via in Situ Electrical Resistance Measurement. *ACS Applied Materials & Interfaces* **2015**, *7*, 25113-25120.
20. Leijtens, T.; Eperon, G. E.; Noel, N. K.; Habisreutinger, S. N.; Petrozza, A.; Snaith, H. J., Stability of Metal Halide Perovskite Solar Cells. *Advanced Energy Materials* **2015**, *5*, 1500963.
21. Li, D.; Bretschneider, S. A.; Bergmann, V. W.; Hermes, I. M.; Mars, J.; Klaseen, A.; Lu, H.; Tremel, W.; Mezger, M.; Butt, H.-J., *et al.*, Humidity-Induced Grain Boundaries in MAPbI₃ Perovskite Films. *The Journal of Physical Chemistry C* **2016**, *120*, 6363-6368.
22. Li, Y.; Xu, X.; Wang, C.; Wang, C.; Xie, F.; Yang, J.; Gao, Y., Degradation by Exposure of Coevaporated CH₃NH₃PbI₃ Thin Films. *The Journal of Physical Chemistry C* **2015**, *119*, 23996-24002.
23. Tong, C.-J.; Geng, W.; Tang, Z.-K.; Yam, C.-Y.; Fan, X.-L.; Liu, J.; Lau, W.-M.; Liu, L.-M., Uncovering the Veil of the Degradation in Perovskite CH₃NH₃PbI₃ Upon Humidity Exposure: A First-Principles Study. *The Journal of Physical Chemistry Letters* **2015**, *6*, 3289-3295.
24. Yang, J.; Siempelkamp, B. D.; Liu, D.; Kelly, T. L., Investigation of CH₃NH₃PbI₃ Degradation Rates and Mechanisms in Controlled Humidity Environments Using in Situ Techniques. *ACS Nano* **2015**, *9*, 1955-1963.
25. Manser, J. S.; Saidaminov, M. I.; Christians, J. A.; Bakr, O. M.; Kamat, P. V., Making and Breaking of Lead Halide Perovskites. *Accounts of Chemical Research* **2016**, *49*, 330-338.
26. Arakcheeva, A.; Chernyshov, D.; Spina, M.; Forro, L.; Horvath, E., CH₃NH₃PbI₃: Precise Structural Consequences of Water Absorption at Ambient Conditions. *Acta Crystallographica Section B* **2016**, *72*, 716-722.
27. Shirayama, M.; Kato, M.; Miyadera, T.; Sugita, T.; Fujiseki, T.; Hara, S.; Kadowaki, H.; Murata, D.; Chikamatsu, M.; Fujiwara, H., Degradation Mechanism of CH₃NH₃PbI₃ Perovskite Materials Upon Exposure to Humid Air. *Journal of Applied Physics* **2016**, *119*, 115501.
28. Han, Y.; Meyer, S.; Dkhissi, Y.; Weber, K.; Pringle, J. M.; Bach, U.; Spiccia, L.; Cheng, Y.-B., Degradation Observations of Encapsulated Planar CH₃NH₃PbI₃ Perovskite Solar Cells at High Temperatures and Humidity. *Journal of Materials Chemistry A* **2015**, *3*, 8139-8147.
29. Niu, G.; Li, W.; Meng, F.; Wang, L.; Dong, H.; Qiu, Y., Study on the Stability of CH₃NH₃PbI₃ Films and the Effect of Post-Modification by Aluminum Oxide in All-Solid-State Hybrid Solar Cells. *Journal of Materials Chemistry A* **2014**, *2*, 705-710.
30. Dong, X.; Fang, X.; Lv, M.; Lin, B.; Zhang, S.; Ding, J.; Yuan, N., Improvement of the Humidity Stability of Organic-Inorganic Perovskite Solar Cells Using Ultrathin Al₂O₃ Layers Prepared by Atomic Layer Deposition. *Journal of Materials Chemistry A* **2015**, *3*, 5360-5367.
31. Hailegnaw, B.; Kirmayer, S.; Edri, E.; Hodes, G.; Cahen, D., Rain on Methylammonium Lead Iodide Based Perovskites: Possible Environmental Effects of Perovskite Solar Cells. *The Journal of Physical Chemistry Letters* **2015**, *6*, 1543-1547.
32. Vincent, B. R.; Robertson, K. N.; Cameron, T. S.; Knop, O., Alkylammonium Lead Halides. Part 1. Isolated PbI₆⁴⁻ Ions in (CH₃NH₃)₄PbI₆ • 2H₂O. *Canadian Journal of Chemistry* **1987**, *65*, 1042-1046.
33. Christians, J. A.; Miranda Herrera, P. A.; Kamat, P. V., Transformation of the Excited State and Photovoltaic Efficiency of CH₃NH₃PbI₃ Perovskite Upon Controlled Exposure to Humidified Air. *Journal of the American Chemical Society* **2015**, *137*, 1530-1538.
34. Wrackmeyer, B., Application of ²⁰⁷Pb NMR Parameters. In *Annual Reports on NMR Spectroscopy*, Academic Press: **2002**; *47*, 1-37.
35. Aliev, A. E.; Law, R. V., Chapter 7 Solid State NMR Spectroscopy. In *Nuclear Magnetic Resonance*, The Royal Society of Chemistry: **2014**; *43*, 286-344.
36. Katz, M. J.; Michaelis, V. K.; Aguiar, P. M.; Yson, R.; Lu, H.; Kaluarachchi, H.; Batchelor, R. J.; Schreckenbach, G.; Kroeker, S.; Patterson, H. H., *et al.*, Structural and Spectroscopic Impact of Tuning the Stereochemical Activity of the Lone Pair in Lead(II) Cyanoaurate Coordination Polymers Via Ancillary Ligands. *Inorganic Chemistry* **2008**, *47*, 6353-6363.

37. Greer, B. J.; Michaelis, V. K.; Katz, M. J.; Leznoff, D. B.; Schreckenbach, G.; Kroeker, S., Characterising Lone-Pair Activity of Lead(II) by ^{207}Pb Solid-State NMR Spectroscopy: Coordination Polymers of $[\text{N}(\text{CN})_2]^-$ and $[\text{Au}(\text{CN})_2]^-$ with Terpyridine Ancillary Ligands. *Chemistry – A European Journal* **2011**, *17*, 3609-3618.
38. Saidaminov, M. I.; Abdelhady, A. L.; Murali, B.; Alarousu, E.; Burlakov, V. M.; Peng, W.; Dursun, I.; Wang, L.; He, Y.; Maculan, G., *et al.*, High-Quality Bulk Hybrid Perovskite Single Crystals within Minutes by Inverse Temperature Crystallization. *Nat Commun* **2015**, *6*, 7586.
39. Halder, A.; Choudhury, D.; Ghosh, S.; Subbiah, A. S.; Sarkar, S. K., Exploring Thermochromic Behavior of Hydrated Hybrid Perovskites in Solar Cells. *The Journal of Physical Chemistry Letters* **2015**, *6*, 3180-3184.
40. Bennett, A. E.; Rienstra, C. M.; Auger, M.; Lakshmi, K. V.; Griffin, R. G., Heteronuclear Decoupling in Rotating Solids. *The Journal of Chemical Physics* **1995**, *103*, 6951-6958.
41. Neue, G.; Dybowski, C.; Smith, M. L.; Hepp, M. A.; Perry, D. L., Determination of $^{207}\text{Pb}^{2+}$ Chemical Shift Tensors from Precise Powder Lineshape Analysis. *Solid State Nuclear Magnetic Resonance* **1996**, *6*, 241-250.
42. Bielecki, A.; Burum, D. P., Temperature Dependence of ^{207}Pb MAS Spectra of Solid Lead Nitrate. An Accurate, Sensitive Thermometer for Variable-Temperature MAS. *Journal of Magnetic Resonance, Series A* **1995**, *116*, 215-220.
43. van Gorkom, L. C. M.; Hook, J. M.; Logan, M. B.; Hanna, J. V.; Wasylishen, R. E., Solid-State Lead-207 NMR of Lead(II) Nitrate: Localized Heating Effects at High Magic Angle Spinning Speeds. *Magnetic Resonance in Chemistry* **1995**, *33*, 791-795.
44. Massiot, D.; Farnan, I.; Gautier, N.; Trumeau, D.; Trokner, A.; Coutures, J. P., ^{71}Ga and ^{69}Ga Nuclear Magnetic Resonance Study of Beta- Ga_2O_3 : Resolution of Four- and Six-Fold Coordinated Ga Sites in Static Conditions. *Solid State Nuclear Magnetic Resonance* **1995**, *4*, 241-248.
45. Nagayama, K.; Bachmann, P.; Wuthrich, K.; Ernst, R. R., The Use of Cross-Sections and of Projections in Two-Dimensional NMR Spectroscopy. *Journal of Magnetic Resonance (1969)* **1978**, *31*, 133-148.
46. Pines, A.; Gibby, M. G.; Waugh, J. S., Proton-Enhanced Nuclear Induction Spectroscopy. A Method for High Resolution NMR of Dilute Spins in Solids. *Journal of Chemical Physics* **1972**, *56*, 1776-1777.
47. Earl, W. L.; Vanderhart, D. L., Measurement of ^{13}C Chemical Shifts in Solids. *Journal of Magnetic Resonance (1969)* **1982**, *48*, 35-54.
48. Eichele, K. *Wsolids NMR Simulation Package*, 1.21.3, Universität Tübingen; **2015**.
49. Forney, C. F.; Brandl, D. G., Control of Humidity in Small Controlled-Environment Chambers Using Glycerol-Water Solutions. *HortTechnology* **1992**, *2*, 52-54.
50. Taylor, R. E.; Beckmann, P. A.; Bai, S.; Dybowski, C., ^{127}I and ^{207}Pb Solid-State NMR Spectroscopy and Nuclear Spin Relaxation in PbI_2 : A Preliminary Study. *The Journal of Physical Chemistry C* **2014**, *118*, 9143-9153.
51. Roiland, C.; Trippe-Allard, G.; Jemli, K.; Alonso, B.; Ameline, J.-C.; Gautier, R.; Bataille, T.; Le Polles, L.; Deleporte, E.; Even, J., *et al.*, Multinuclear NMR as a Tool for Studying Local Order and Dynamics in $\text{CH}_3\text{NH}_3\text{PbX}_3$ (X = Cl, Br, I) Hybrid Perovskites. *Physical Chemistry Chemical Physics* **2016**, *18*, 27133-27142.
52. Rosales, B. A.; Men, L.; Cady, S. D.; Hanrahan, M. P.; Rossini, A. J.; Vela, J., Persistent Dopants and Phase Segregation in Organolead Mixed-Halide Perovskites. *Chemistry of Materials* **2016**, *28*, 6848-6859.
53. Wasylishen, R., *private communication*, **2016**.
54. Onoda-Yamamuro, N.; Matsuo, T.; Suga, H., Calorimetric and Ir Spectroscopic Studies of Phase Transitions in Methylammonium Trihalogenoplumbates (II) $^+$. *Journal of Physics and Chemistry of Solids* **1990**, *51*, 1383-1395.
55. Knop, O.; Wasylishen, R. E.; White, M. A.; Cameron, T. S.; Oort, M. J. V., Alkylammonium Lead Halides. Part 2. $\text{CH}_3\text{NH}_3\text{PbX}_3$ (X = Cl, Br, I) Perovskites: Cuboctahedral Halide Cages with Isotropic Cation Reorientation. *Canadian Journal of Chemistry* **1990**, *68*, 412-422.
56. Wasylishen, R. E.; Knop, O.; Macdonald, J. B., Cation Rotation in Methylammonium Lead Halides. *Solid State Communications* **1985**, *56*, 581-582.

57. Weller, M. T.; Weber, O. J.; Henry, P. F.; Di Pumpo, A. M.; Hansen, T. C., Complete Structure and Cation Orientation in the Perovskite Photovoltaic Methylammonium Lead Iodide between 100 and 352 K. *Chemical Communications* **2015**, *51*, 4180-4183.
58. Imler, G. H.; Li, X.; Xu, B.; Dobereiner, G. E.; Dai, H.-L.; Rao, Y.; Wayland, B. B., Solid State Transformation of the Crystalline Monohydrate $(\text{CH}_3\text{NH}_3)\text{PbI}_3(\text{H}_2\text{O})$ to the $(\text{CH}_3\text{NH}_3)\text{PbI}_3$ Perovskite. *Chemical Communications* **2015**, *51*, 11290-11292.
59. Wakamiya, A.; Endo, M.; Sasamori, T.; Tokitoh, N.; Ogomi, Y.; Hayase, S.; Murata, Y., Reproducible Fabrication of Efficient Perovskite-Based Solar Cells: X-Ray Crystallographic Studies on the Formation of $\text{CH}_3\text{NH}_3\text{PbI}_3$ Layers. *Chemistry Letters* **2014**, *43*, 711-713.
60. Zhao, J.; Cai, B.; Luo, Z.; Dong, Y.; Zhang, Y.; Xu, H.; Hong, B.; Yang, Y.; Li, L.; Zhang, W., *et al.*, Investigation of the Hydrolysis of Perovskite Organometallic Halide $\text{CH}_3\text{NH}_3\text{PbI}_3$ in Humidity Environment. *Scientific Reports* **2016**, *6*, 21976.
61. Wang, B.; Chen, T., Exceptionally Stable $\text{CH}_3\text{NH}_3\text{PbI}_3$ Films in Moderate Humid Environmental Condition. *Advanced Science* **2016**, *3*, 1500262.
62. Brivio, F.; Frost, J. M.; Skelton, J. M.; Jackson, A. J.; Weber, O. J.; Weller, M. T.; Goni, A. R.; Leguy, A. M.; Barnes, P. R.; Walsh, A., Lattice Dynamics and Vibrational Spectra of the Orthorhombic, Tetragonal, and Cubic Phases of Methylammonium Lead Iodide. *Physical Review B* **2015**, *92*, 144308.

TOC Graphic

